Supporting Information for

A Chlorin-based Nanoscale Metal-Organic Framework Systemically Rejects Colorectal Cancers via Synergistic Photodynamic Therapy and Checkpoint Blockade Immunotherapy

Kuangda Lu,[a, †] Chunbai He,[a, †] Nining Guo,[a,b] Christina Chan,[a] Kaiyuan Ni,[a] Ralph R. Weichselbaum,[b] Wenbin Lin[a,*]

[a]*Department of Chemistry, The University of Chicago, Chicago, IL 60637, USA;*
[b]*Department of Radiation and Cellular Oncology and The Ludwig Center for Metastasis Research, The University of Chicago, Chicago, IL 60637, USA;*
E-mail: wenbinlin@uchicago.edu

Table of Contents

1. Supplementary methods

Synthesis of TBP-Hf: To a 2-dram glass vial was added 1 mL of $HfCl_4$ solution [2 mg/mL in N,N-diethylformamide (DEF), 6.2 μmol], 1 mL of the H_4TBP solution (1.9 mg/mL in DEF, 2.4 μmol), and 60 mg of benzoic acid (0.49 mmol). The reaction mixture was kept in a 120 °C oven for 2 days. The violet powder was collected by centrifugation and washed with DMF, 1% triethylamine in ethanol (v/v), and ethanol.

Powder X-ray diffraction: TBC-Hf or TBP-Hf sample was prepared by centrifugation in a capillary tube with one end sealed. The powder X-ray diffraction pattern was acquired on Bruker D8 VENTURE single crystal dual-source diffractometer (Bruker, Germany) and integrated with the Bruker software.

BET surface area measurement: Nitrogen adsorption of TBC-Hf and TBP-Hf was performed on 3Flex-Surface Characterization Analyzer (Micromeritics, USA) at 77K (Figure S7). The BET surface areas were calculated to be 1077 and 1462 m^2/g.

Digestion for ICP-MS: The nMOF samples was dried under vacuum overnight before being digested by a mixture of concentrate nitric acid and hydrofluoric acid (63% HF/69% HNO_3 1/100 v/v). The sample was diluted 35 times and filtered by a PES syringe filter unit before ICP-MS analysis.

Thermogravimetric analysis: Thermogravimetric analysis on TBC-Hf was carried out on a Shimadzu TGA-50 thermogravimetric analyzer. The nMOF was collected by centrifugation and dried under vacuum overnight. The sample was then transferred to a platinum pan and heated at 3 °C/min to 650 °C in air. The weight percentage was plotted against temperature and was normalized to the weight at 150 °C to eliminate the influence of absorbed moisture.

Fluorescence measurement: The fluorescence spectra were taken on a spectrofluorophotometer (Fluorolog-3, Horiba, Japan). Samples were prepared as 1 μM solutions in phosphate buffer saline or water by equivalent ligand concentration for the measurements.

Fluorescence lifetime measurement: Time-domain lifetimes were measured on a ChronosBH lifetime fluorometer (ISS, Inc.) using Time-Correlated Single Photon Counting (TCSPC) methods. The fluorimeter contained Becker-Hickl SPC-130 detection electronics and an HPM-100-40 Hybrid PMT detector. Excitation was provided by a 403 nm picosecond pulsed laser source (Hamamatsu PLP-10). Emission wavelengths were selected with interference filters (Semrock). The Instrument Response Function (IRF) was measured to be approximately 0.009 ns FWHM in a 1% scattering solution of Ludox LS colloidal silica. Multi-component exponential decay lifetimes were fit via a forward convolution method in the Vinci control and analysis software. Samples were prepared into solution/suspensions in water for measurements.

Cellular uptake evaluation: TBP-Hf or TBC-Hf was incubated with CT26 cells at a Hf concentration of 150 μM for 24 h. The cells were collected, counted with a hemocytomter, and digested by concentrated nitric acid. The cellular uptake amounts of Hf were determined by ICP-MS and normalized with cell numbers.

IDOi encapsulation: To a suspension of TBC-Hf in ethanol (2.5 mg/mL, 3.0 mL), 3.3 mg of IDOi was added. The mixture was sonicated for 1 minute and 3.0 mL of water was added. The solution was stirred at room temperature in the dark for 12 h to afford IDOi@TBC-Hf. IDOi@TBC-Hf was collected by centrifugation and washed with 50% ethanol/water.

IDOi@TBC-Hf drug release profile: IDOi@TBC-Hf was suspended in Hank's balanced salt solution (HBSS, 2.5 mg of IDOi@TBC-Hf in 10 mL of HBSS). The suspension was added to a dialysis bag (3500 molecular weight cut-off) and dialyzed in another 190 mL of HBSS (total 200 mL) in a beaker. At 10 min, 30 min, 1 h, 2 h, 6 h and

24 h of dialysis 2.00 mL of the solution was taken from the beaker while 2 mL of fresh HBSS was added to the beaker. The samples were freeze-dried to off-white powders, dissolved in 2.00 mL of HPLC-grade methanol and filtered through 0.2 μm PTFE filter unit for LC-MS determination.

LC-MS/MS analysis was conducted using an Agilent Zorbax SB-C18 (50×2.1 mm, 5 μm) column at 25 °C. The mobile phases were 0.2% formic acid in water v/v (A) and acetonitrile (B). The elution gradient was as follows: hold at 0% B for 1.5 min, to 40% B in 1.5 min, hold at 40% B for 4 min, to 0% B in 1.5 min, hold at 0% B for 2 min. Samples were stored in methanol and held at 4°C during analysis.

2. Synthesis of 5,10,15,20-tetra(p-benzoato)chlorin (H_4TBC)

Synthesis of 5,10,15,20-tetra(p-methylbenzoato)porphyrin (Me_4TBP)

A mixture of 6.83 g of methylterephthalaldehydate (41.6 mmol) and 2.80 mL of pyrrole (40.4 mmol) was dissolved in 100 mL of propionic acid. The solution was heated to reflux (150 °C) in the dark overnight. The purple product was collected by vacuum filtration and was sequentially washed with water, methanol and ethyl ether. Yield: 24.3%. ^{1}H NMR (500 MHz, $CDCl_3$, ppm, Figure S1): δ=8.84 (s, 8H), 8.47 (d, 8H), 8.32 (d, 8H), 4.14 (s, 12H), -2.79 (s, 2H).

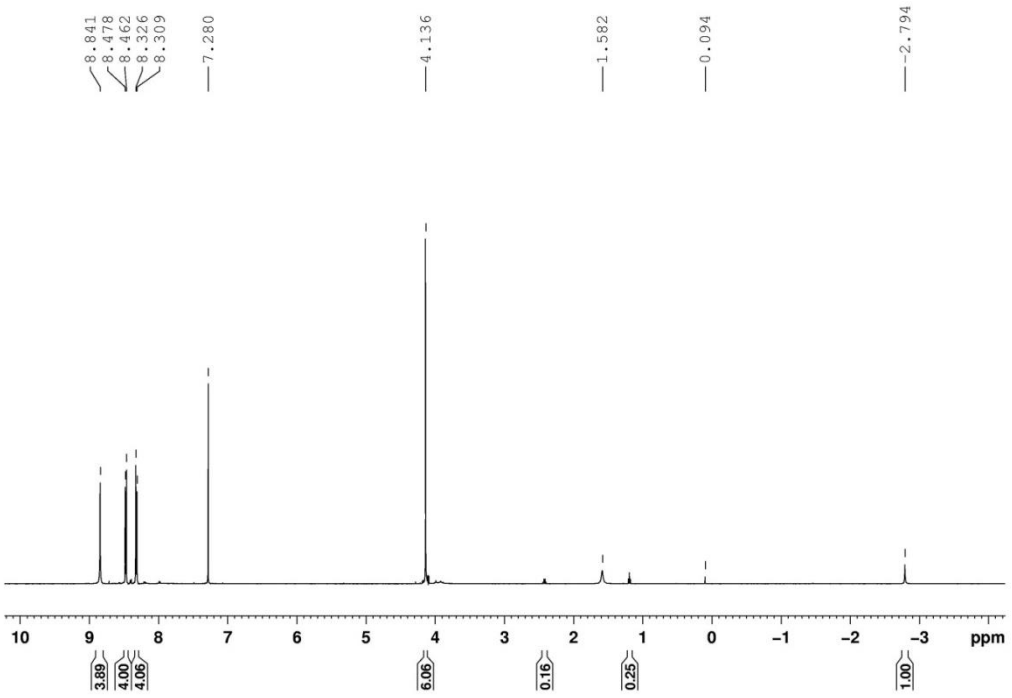

Figure S1. ^{1}H NMR of 5,10,15,20-tetra(p-methylbenzoato)porphyrin.

Synthesis of 5,10,15,20-tetra(p-methylbenzoato)chlorin (Me_4TBC)

Me_4TBP (500 mg, 0.59 mmol) and anhydrous potassium carbonate (750 mg, 5.4 mmol) were added to a 2-neck round bottom flask. 40 mL of anhydrous pyridine was added under nitrogen. The solution was heated to 105 °C before the addition of 4.0 mL of p-toluenesulfonhydrazide solution (0.30 M in anhydrous pyridine). The reaction mixture was kept at 105 °C for 4 hours during which another 2 fractions of p-toluenesulfonhydrazide solutions (0.30 M in anhydrous pyridine, 4.0 mL for each fraction) were added every 2 h. The reaction mixture was then stirred at 105 °C in the dark for another 12 h. The product was extracted with 2:1 ethyl acetate/water and washed with 2 M HCl, 2 M phosphoric acid, water, and saturated sodium bicarbonate solution. The solution was treated with 2,3-dichloro-5,6-dicyano-benzoquinone (via slow addition of 1 mg/mL solution in chloroform) until the characteristic absorption of the over-reduced product at ~735 nm disappeared. The product was purified by aluminum oxide column chromatography with dichloromethane as the eluent. Yield: 16%. ESI-MS for $[Me_4TBC+H]^+$: 849.3 calcd, 849.4 found (Figure S2). ^1H NMR (500 MHz, $CDCl_3$, ppm, Figure S3): δ=8.57 (d, 2H), 8.40 (m, 10H), 8.20 (m, 6H), 7.99 (d, 4H), 4.18 (s, 4H), 4.11 (s, 6H), 4.09 (s, 6H), -1.45 (s, 2H).

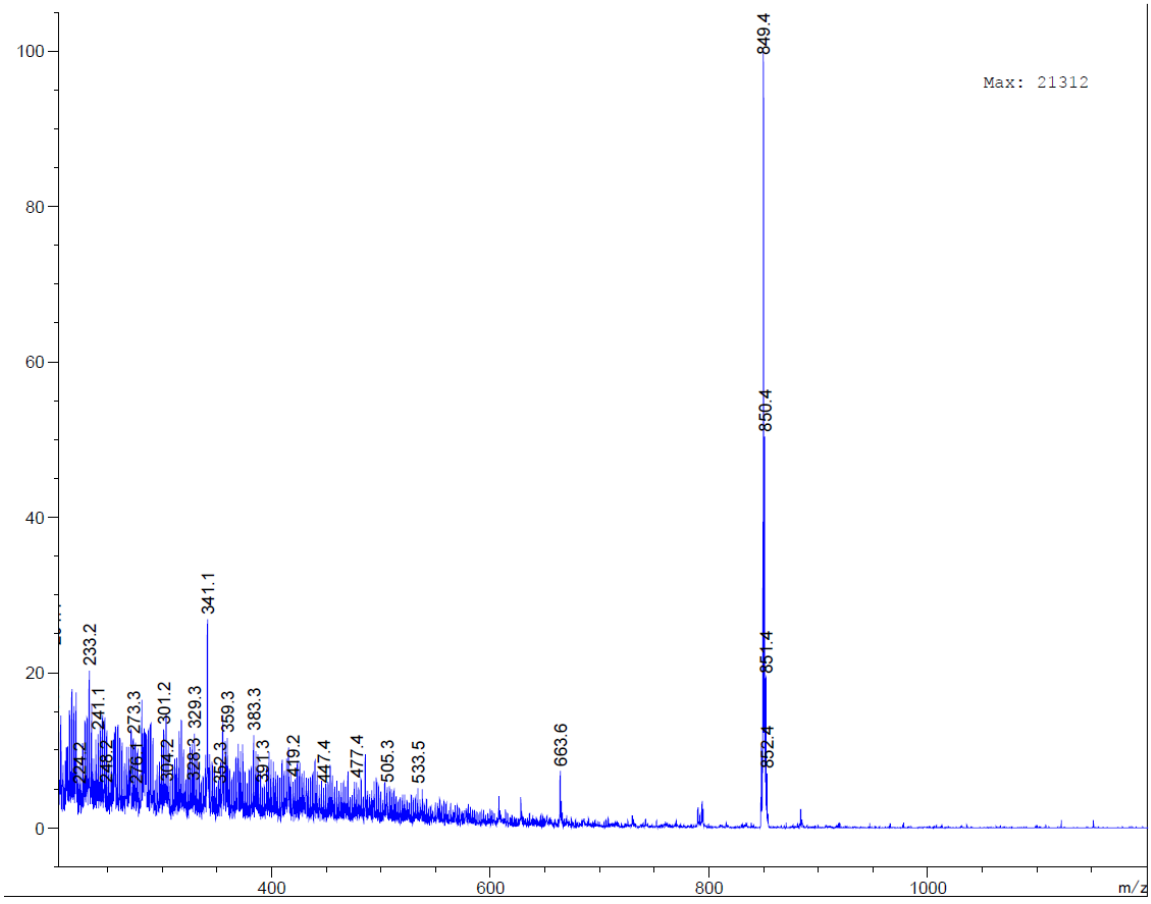

Figure S2. ESI-MS of 5,10,15,20-tetra(p-methylbenzoato)chlorin. The sample was prepared in chloroform as a 50 mg/L solution and was delivered by methanol.

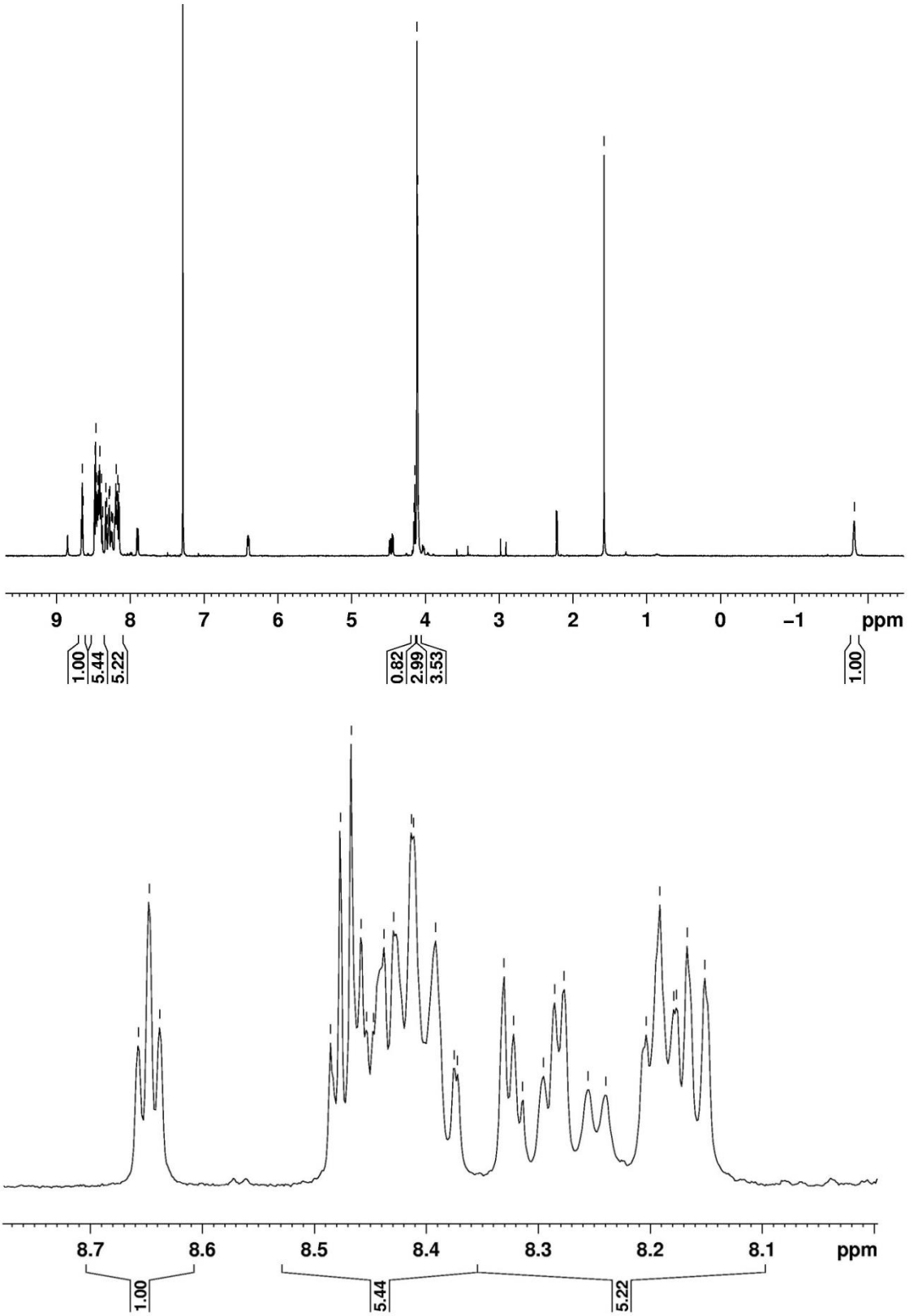

Figure S3. Top, ^{1}H NMR of 5,10,15,20-tetra(p-methylbenzoato)chlorin. Bottom, the expanded view of a portion of the spectrum.

Synthesis of 5,10,15,20-tetra(p-benzoato)chlorin (H_4TBC)

The hydrolysis of Me_4TBC was conducted in 1:1 THF/methanol under N_2. An aqueous NaOH solution (2 mol/L, 40 equiv.) was added to a solution of Me_4TBC after degasing with N_2. The solution was heated at 74 °C (reflux) overnight. After removing most of the organic volatile by a rotary evaporator, the solution was diluted with water and acidified with HCl (1 M) to pH=3. The product was collected by vacuum filtration and washed with water and methanol before drying under vacuum. Yield: 78%. ESI-MS for $[H_4TBC+H]^+$: 793.2 calcd, 793.3 found (Figure S4). ^{1}H NMR (500 MHz, DMSO-d_6, ppm, Figure S5): δ=8.60 (d, 2H), 8.40-8.29 (m, 12H), 8.19 (m, 4H), 8.01 (d, 4H), 4.10 (s, 4H), -1.56 (s, 2H).

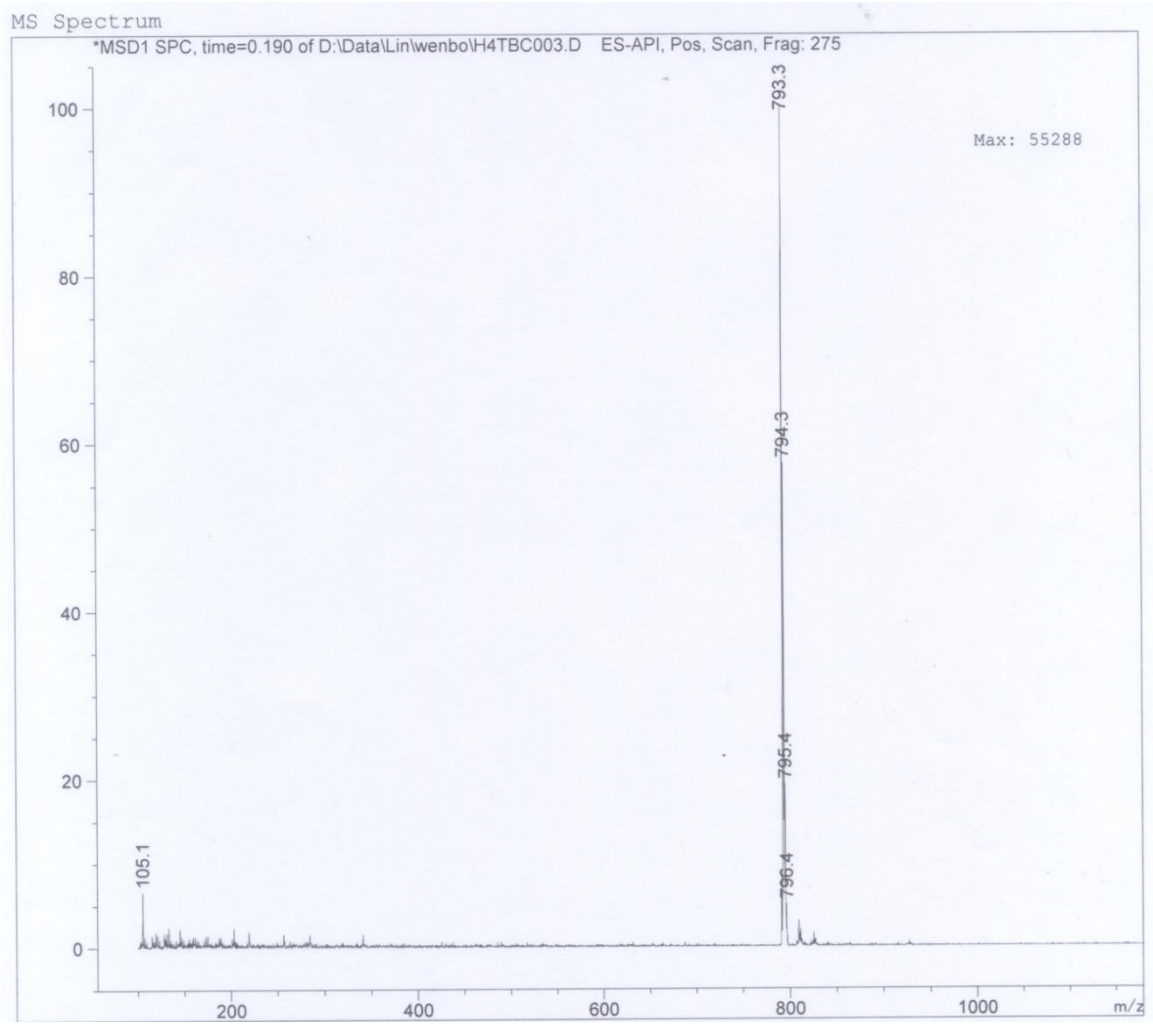

Figure S4. ESI-MS of 5,10,15,20-tetra(p-benzoato)chlorin. The sample was prepared in DMSO as a 50 mg/L solution and was delivered by methanol.

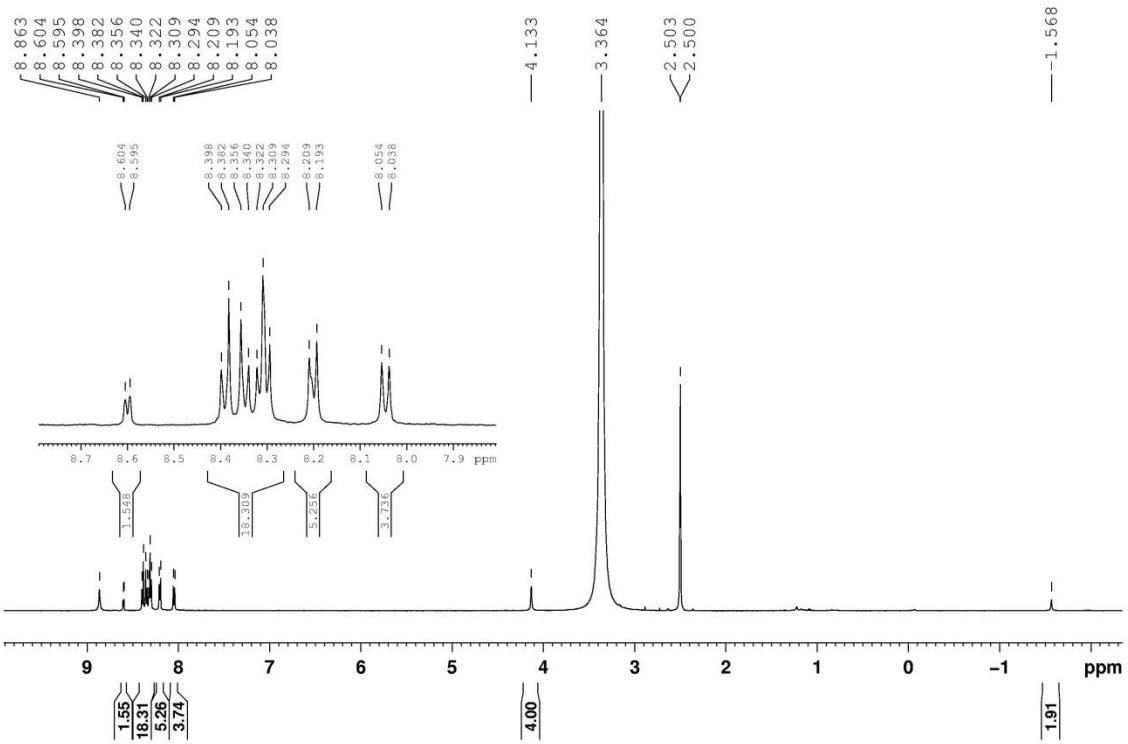

Figure S5. ^{1}H NMR of 5,10,15,20-tetra(p-benzoato)chlorin. Inset is the expanded view of a portion of the spectrum.

3. Characterization of TBP-Hf and TBC-Hf

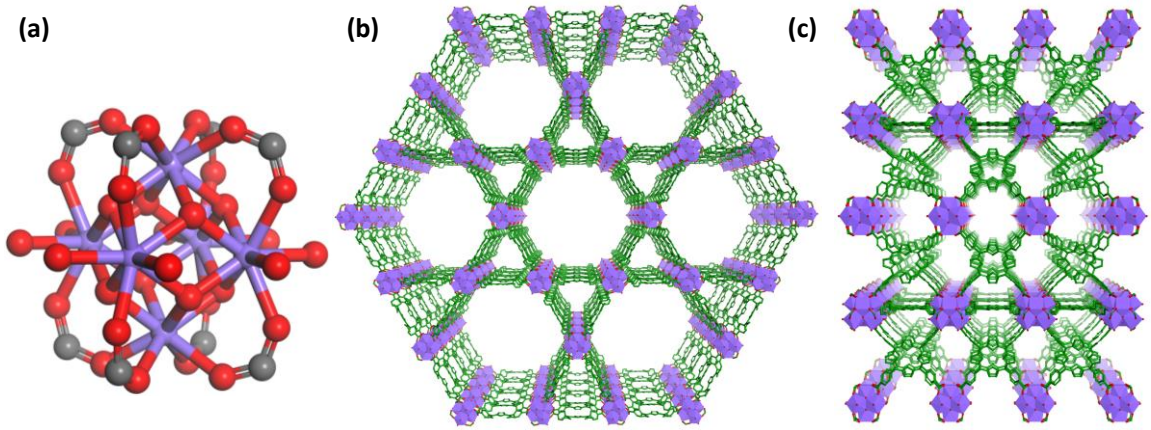

Figure S6. Structure model of TBC-Hf. (a) The secondary building unit (SBU) of TBC-Hf (Violet, Hf; red, O; gray, C). (b-c) The view of the TBC-Hf structure along the [001] (b) and [100] (c) direction.

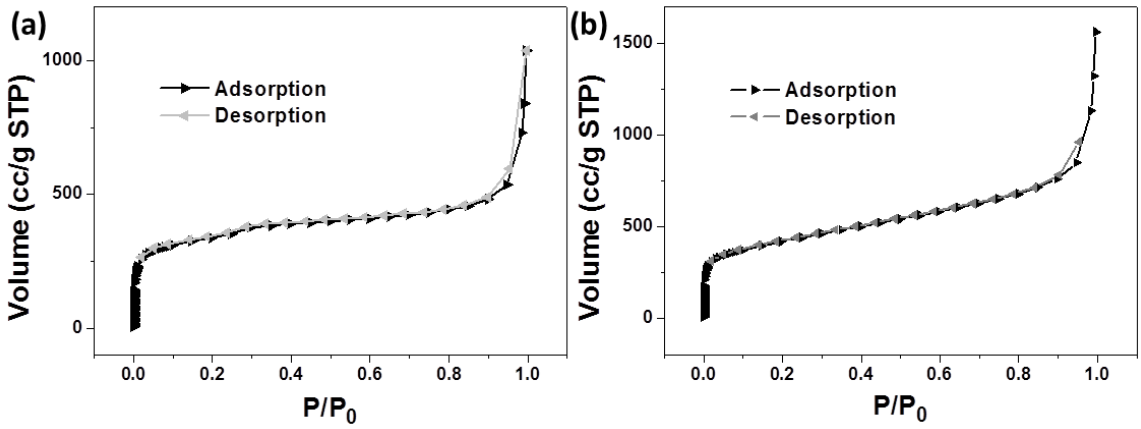

Figure S7. Nitrogen adsorption isotherms of TBC-Hf (a) and TBP-Hf (b) at 77K.

The morphologies of TBP-Hf and TBC-Hf were confirmed by transmission electron microscopy (TEM, Tecnai F30 and Tecnai Spirit, FEI, USA) and the distances of lattice fringes were measured as shown in Figure S8-S9. TBP-Hf displays a rod-like morphology with a width of 20-30 nm and a length of ~100 nm. TBC-Hf is rice-shaped with a typical width of 30-60 nm and a length of 60-120 nm. Particle sizes of TBP-Hf and TBC-Hf were determined to be 72.7 nm (PDI=0.085) and 83.2 nm (PDI=0.071), respectively, by dynamic light scattering (DLS, Nano-ZS, Malvern, UK; Figure S10).

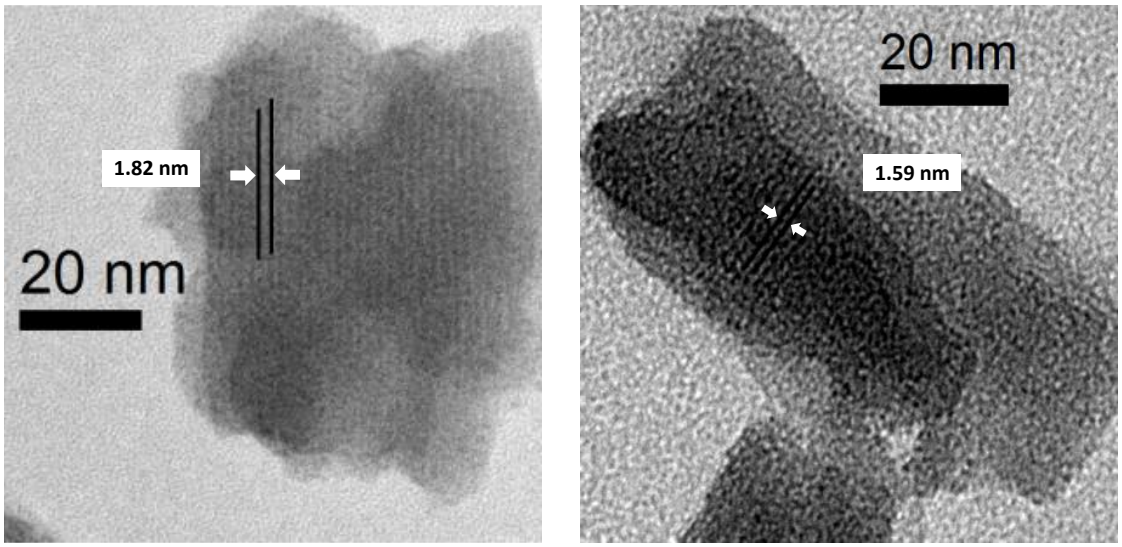

Figure S8. High resolution TEM showing the lattice fringes of TBP-Hf in different directions.

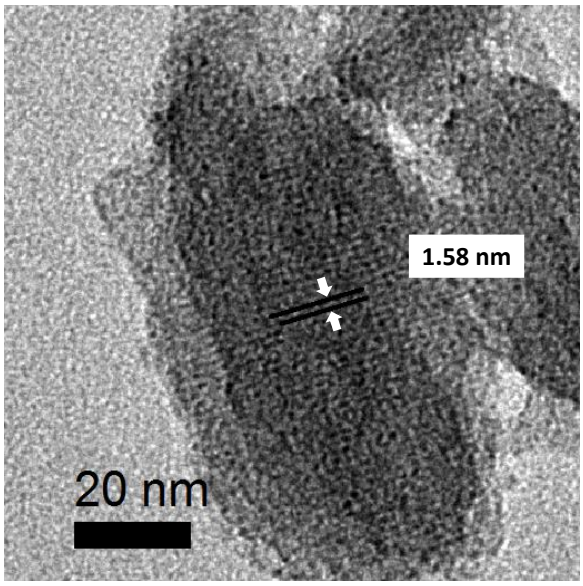

Figure S9. High resolution TEM showing the lattice fringes of TBC-Hf.

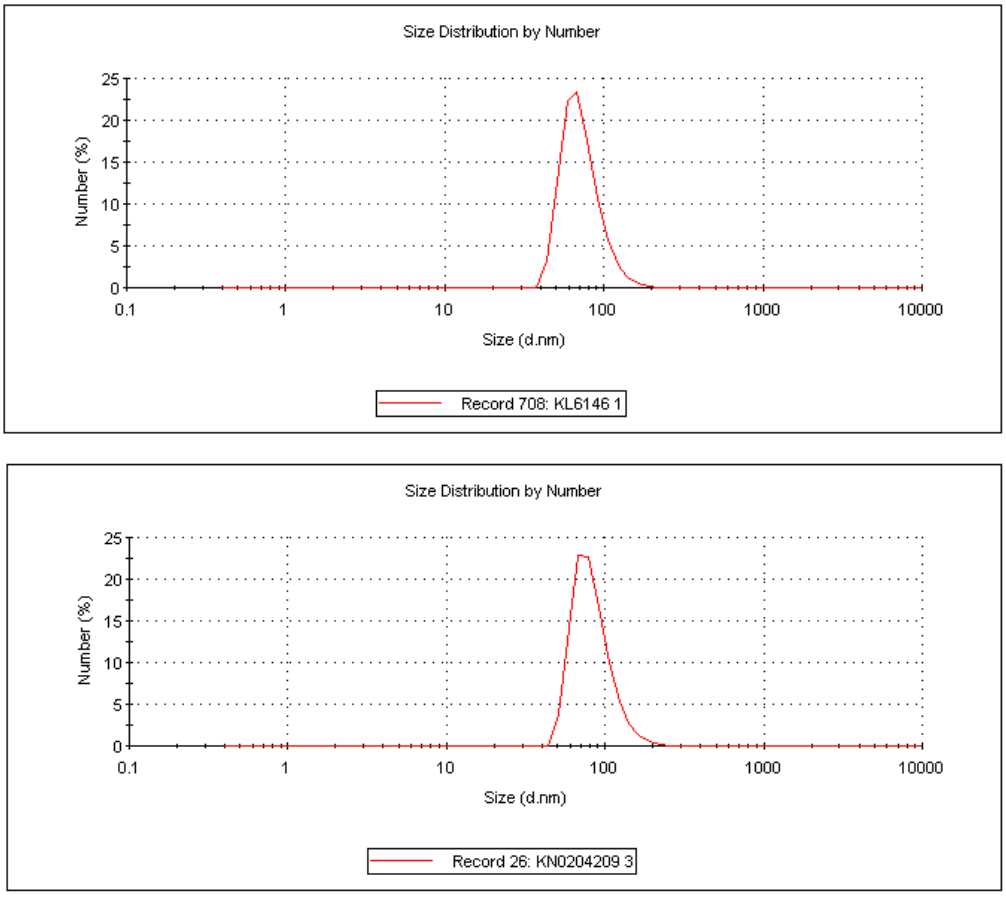

Figure S10. DLS plots showing the particle sizes of TBP-Hf (top) and TBC-Hf (bottom).

Thermogravimetric analysis of TBC-Hf was carried out on Shimadzu TGA-50 thermogravimetric analyzer. The heating rate was set to 3 °C/min and the sample was heated to 650 °C in air. The weight percentage was plotted against temperature (Figure S11a). The normalized percent weight loss from 150 °C to 650 °C was 61.7% for TBC-Hf, which corresponded to the calculated TBC ligand weight loss based on the MOF formula (56.8%). The IDOi loading was calculated to be 4.7% by weight following the equation below:

$$loading\ wt\% = \left(1 - \frac{remaining\ wt\%\ after\ loading}{remaining\ wt\%\ before\ loading}\right) \times 100\%$$

The IDOi loading was also confirmed by ^{1}H NMR after digestion by K_3PO_4/D_2O and extraction with DMSO-d_6. The NMR-determined IDOi loading is 4.3% by weight (IDOi:TBC=0.24 by mol, Figure S11c), consistent to the TGA-quantified IDOi loading of 4.7% by weight (IDOi:TBC=0.26 by the molar ratio).

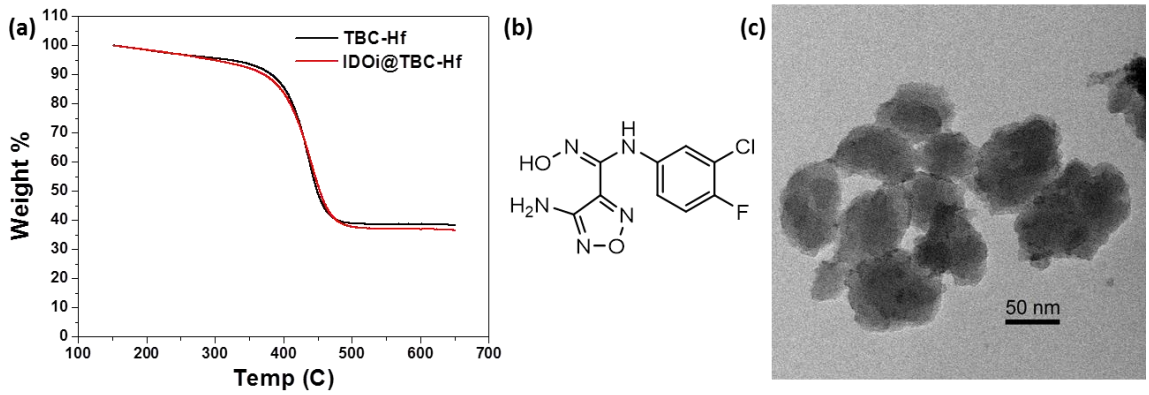

Figure S11. (a) TGA of TBC-Hf before and after IDOi loading. (b) The chemical structure of the IDOi 4-amino-N-(3-chloro-4-fluoro-phenyl)-N'-hydroxy-1,2,5-oxadiazole-3-carboximidamide. (c) TEM image of IDOi@TBC-Hf.

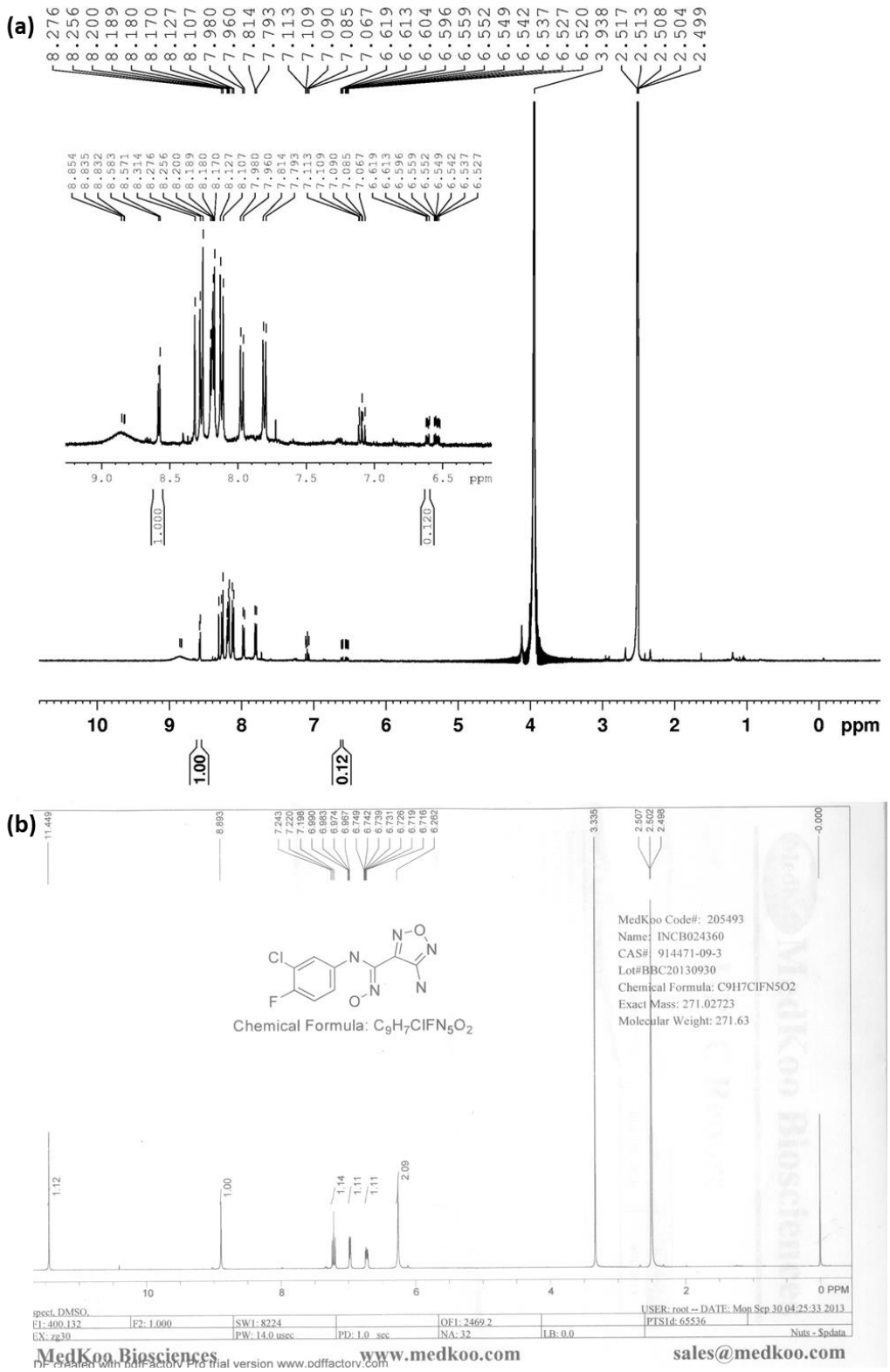

Figure S12. (a) ^{1}H NMR spectrum of IDOi@TBC-Hf digestion in DMSO-d_6. (b) The ^{1}H NMR spectrum of IDOi in DMSO-d_6, provided by the vendor.

The release of IDOi was studied by dialysis in Hank's balanced salt solution (HBSS). IDOi released almost linearly in the first 6 hours, and then slowed down. At 24 h of dialysis 83.3% of IDOi was released.

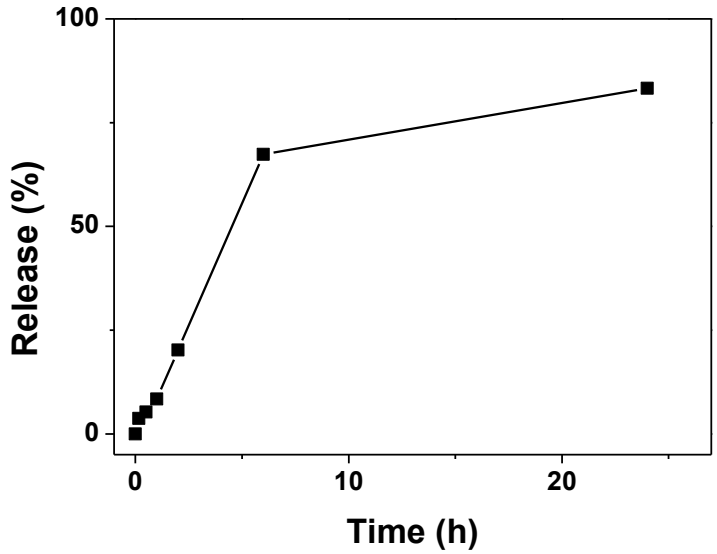

Figure S13. Release of IDOi from IDOi@TBC-Hf in HBSS by dialysis.

4. Photophysical properties

The UV-visible absorption spectra of H_4TBP, H_4TBC, TBP-Hf, and TBC-Hf were acquired with a UV-vis spectrophotometer (UV-2401PC, Shimadzu, Japan). The ligands and the nMOFs were prepared as 3 μM (for PS concentration) solutions/suspensions in dimethyl sulfoxide or ethanol. The extinction coefficients of H_4TBP and H_4TBC at 420 nm (Soret band) are 4.60×10^5 $M^{-1}cm^{-1}$ and 3.81×10^5 $M^{-1}cm^{-1}$, respectively. The extinction coefficients of TBP-Hf and TBC-Hf Soret peaks are 3.59×10^5 $M^{-1}cm^{-1}$ and 2.92×10^5 $M^{-1}cm^{-1}$, respectively. For the nMOFs, the apparent extinction coefficients could be influenced by scattering and broadening of Soret peaks.

The fluorescence spectra of ligands and nMOFs were taken on a spectrofluoro-photometer (Fluorolog-3, Horiba, Japan). The samples were prepared as 1 μM solutions (based on PS concentration) in phosphate buffer saline (PBS) or water. H_4TBP, H_4TBC, TBP-Hf and TBC-Hf were prepared as solution/suspensions in PBS or water. The fitted lifetimes are listed in Table S1.

Table S1 Lifetimes of H_4TBP, H_4TBC, TBP-Hf and TBC-Hf fluorescence in different media, fitted by software.

sample	τ (ns)	χ^2
H_4TBP _PBS	9.25±0.05	1.05
TBP-Hf _water	8.38±0.04	1.65
H_4TBC _PBS	9.56±0.01	2.22
TBC-Hf_water	8.25±0.01	1.08

5. Singlet oxygen generation

A light-emitting diode (LED) array with peak emission at 650 nm was used as the light source for singlet oxygen generation. The irradiance of LED was 20 mW/cm^2. Singlet oxygen sensor green (SOSG) reagent (Life Technologies) was employed to detect singlet oxygen. H_4TBP, H_4TBC, TBP-Hf and TBC-Hf samples were prepared in 1 μM solutions/suspensions in water (for the nMOFs, the concentration was calculated as ligand equivalents). To 2 mL of these solutions/suspensions, SOSG stock solution (5 μL at 5 mM) was added (final concentration=12.5 μM) before fluorescence measurement.

For a typical measurement, fluorescence intensity was acquired on a spectrofluorophotometer (RF-5301PC, Shimadzu, Japan) with excitation at 504 nm and emission at 525 nm (slit width 1.5 nm/3 nm for ex/em). Fluorescence was measured after irradiation by LED for 0 (as background), 0.5, 1, 1.5, 2, 3, 4, 5, 7 and 10 min.

6. In vitro cellular uptake, cytotoxicity and mechanistic studies

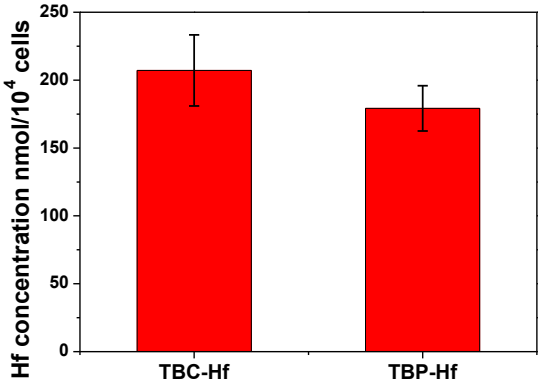

Figure S14. Cellular uptake of TBP-Hf and TBC-Hf by CT26 cells.

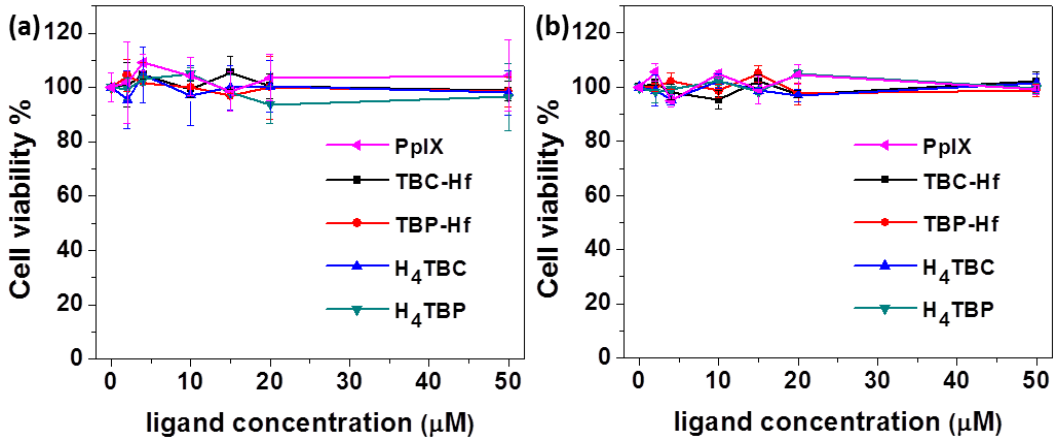

Figure S15. Cell viability of the dark control groups on CT26 (a) or MC38 (b) cells.

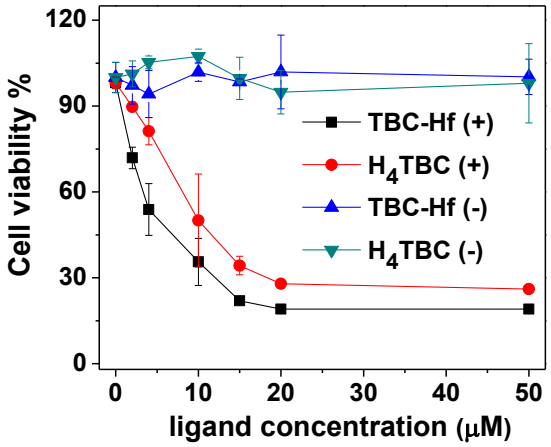

Figure S16. *In vitro* PDT efficacy of TBC-Hf and H_4TBC on B16F10 cells.

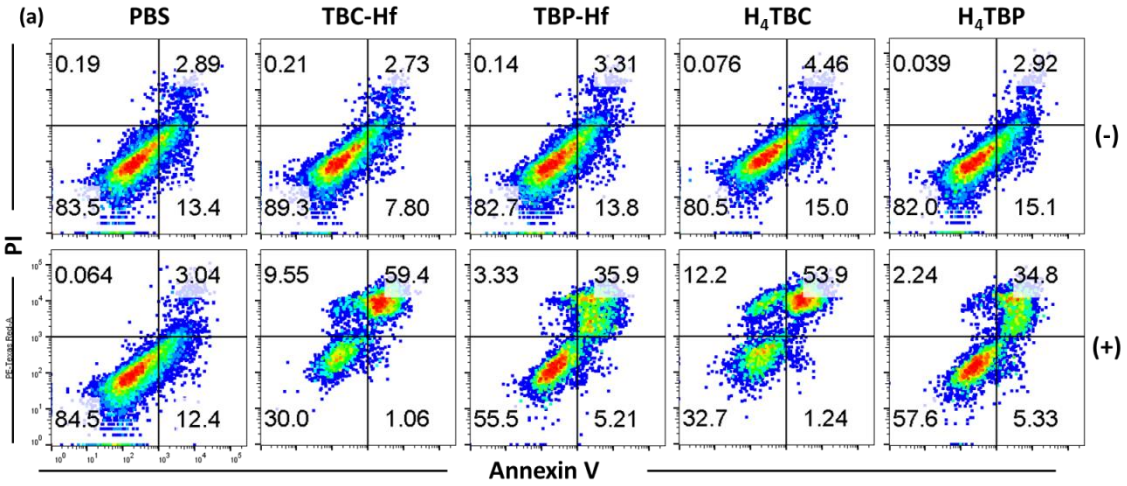

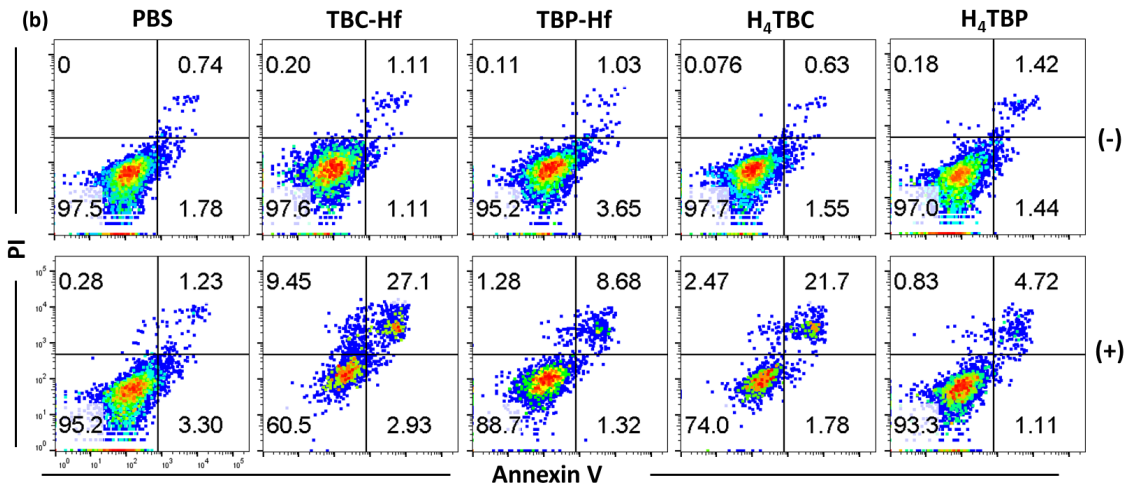

Figure S17. Annexin V/PI analysis of CT26 (a) and MC38 (b) cells incubated with PBS, TBC-Hf, TBP-Hf, H_4TBC and H_4TBP with or without irradiation (90 J/cm^2). The quadrants from lower left to upper left (counter clockwise) represent healthy, early apoptotic, late apoptotic, and necrotic cells, respectively. The percentage of cells in each quadrant was shown on the graphs. (+) and (-) refer to with and without irradiation, respectively.

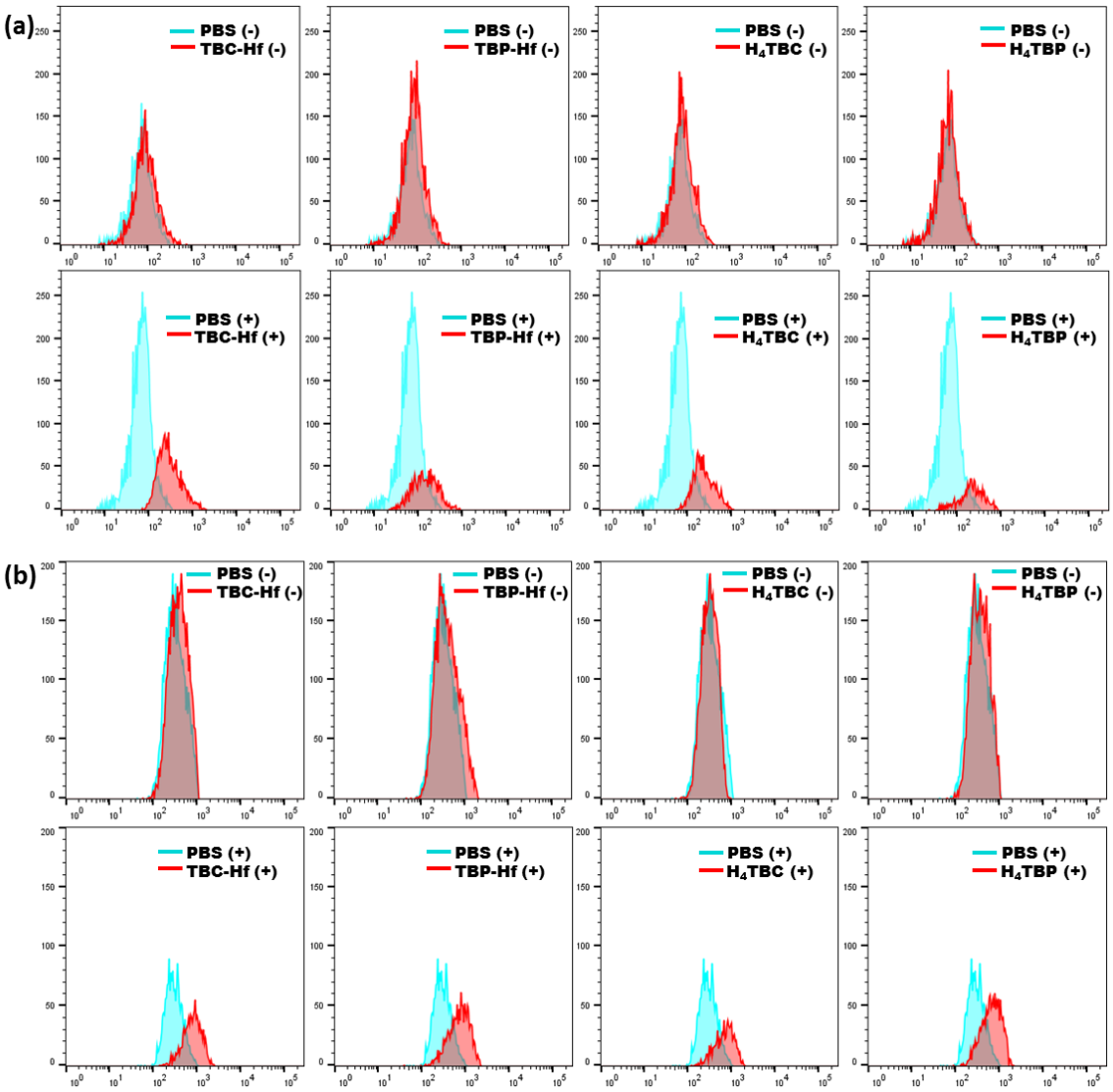

Figure S18. CRT exposure on the cell surface of CT26 (a) and MC38 (b) was assessed after incubation with PBS, TBC-Hf, TBP-Hf, H_4TBC and H_4TBP, with (+) or without (-) light irradiation (90 J/cm^2) by flow cytometry analysis. The fluorescence intensity was gated on PI-negative cells.

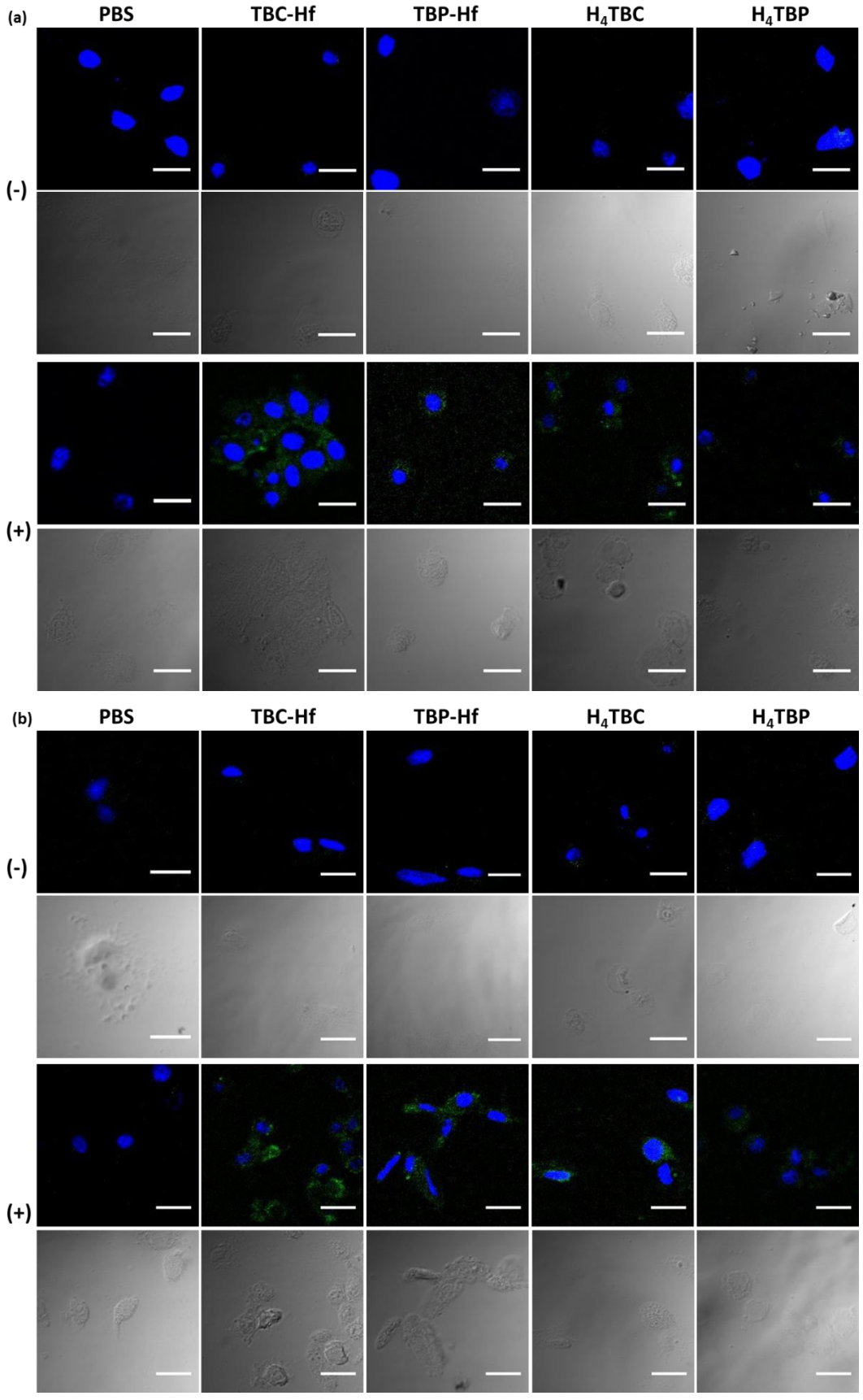
(a)
PBS
TBC-Hf
TBP-Hf
H4TBC
H4TBP
(-)
(+)
(b)
PBS
TBC-Hf
TBP-Hf
H4TBC
H4TBP
(-)
(+)

Figure S19. Immunofluorescence microscopy of CRT expression on the cell surface of CT26 (a) and MC38 (b) treated with PBS, TBC-Hf, TBP-Hf, H_4TBC and H_4TBP with (+) or without (-) irradiation (90 J/cm^2). Scale bar = 50 μM.

7. In vivo studies on combined PDT and immunotherapy

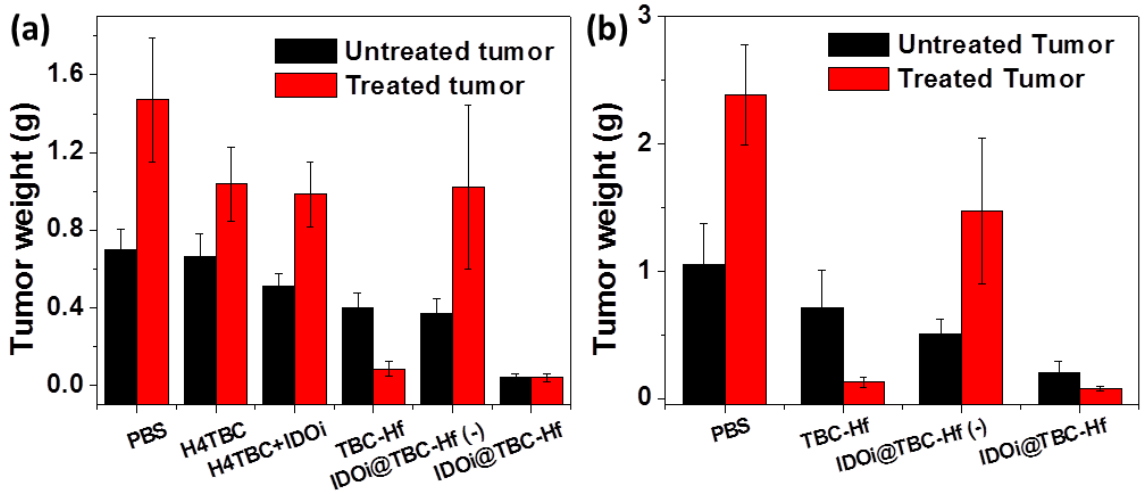

Figure S20. Tumor weights after PDT treatment on CT26 (a) and MC38 (b) models. Data collected after euthanizing the mice on day 10.

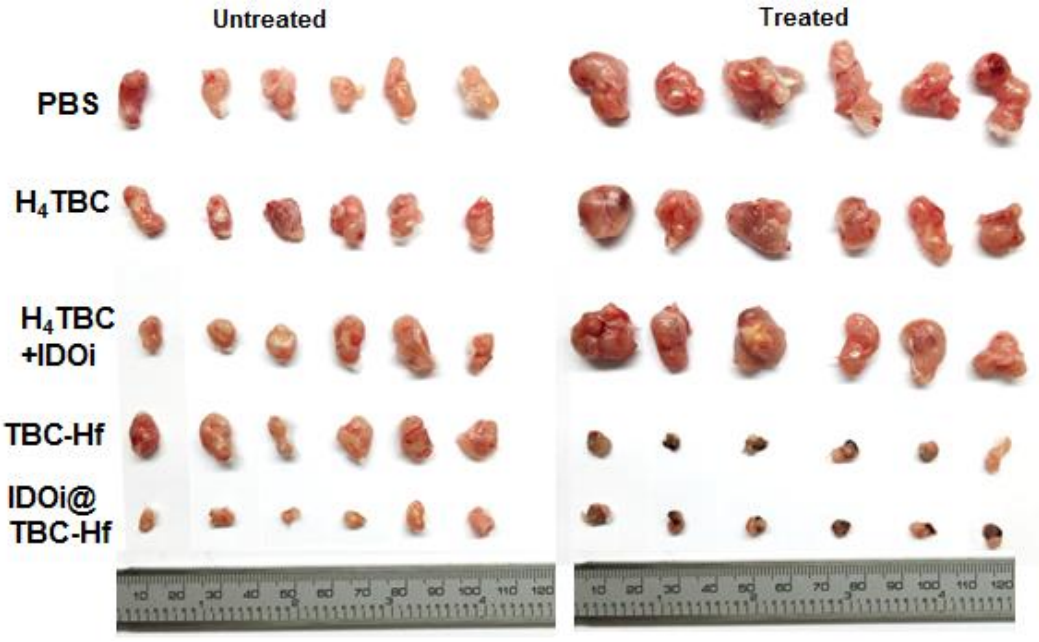

Figure S21. Photos of excised tumors of each group after PDT treatment in the CT26 model.

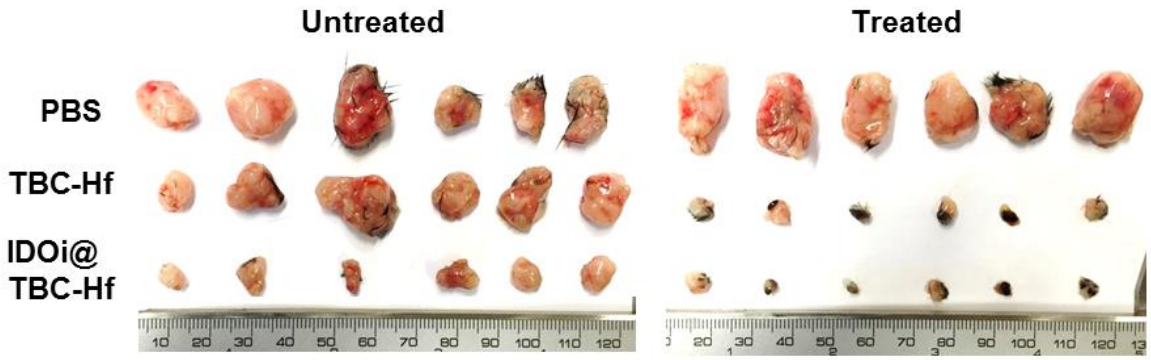

Figure S22. Photos of excised tumors of each group after PDT treatment in the MC38 model.

Table S2 Statistical analysis of the tumor sizes at the end of treatment on CT26 tumor bearing mice.

	P values	
	Treated tumor	Untreated tumor
PBS vs H_4TBC	0.0098	0.0011
PBS vs H_4TBC+IDOi	< 0.0001	0.0002
PBS vs TBC-Hf	< 0.0001	< 0.0001
PBS vs IDOi@TBC-Hf (-)	0.34	0.0005
PBS vs IDOi@TBC-Hf	< 0.0001	< 0.0001
TBC-Hf vs IDOi@TBC-Hf	0.17	< 0.0001
IDOi@TBC-Hf (-) vs (+)	< 0.0001	< 0.0001

Table S3 Statistical analysis of the tumor sizes at the end of treatment on MC38 tumor bearing mice.

	P values	
	Treated tumor	Untreated tumor
PBS vs TBC-Hf	< 0.0001	0.0005
PBS vs IDOi@TBC-Hf (-)	0.19	< 0.0001
PBS vs IDOi@TBC-Hf	< 0.0001	< 0.0001
TBC-Hf vs IDOi@TBC-Hf	0.81	<0.0001
IDOi@TBC-Hf (-) vs (+)	< 0.0001	< 0.0001

8. Immunoanalysis

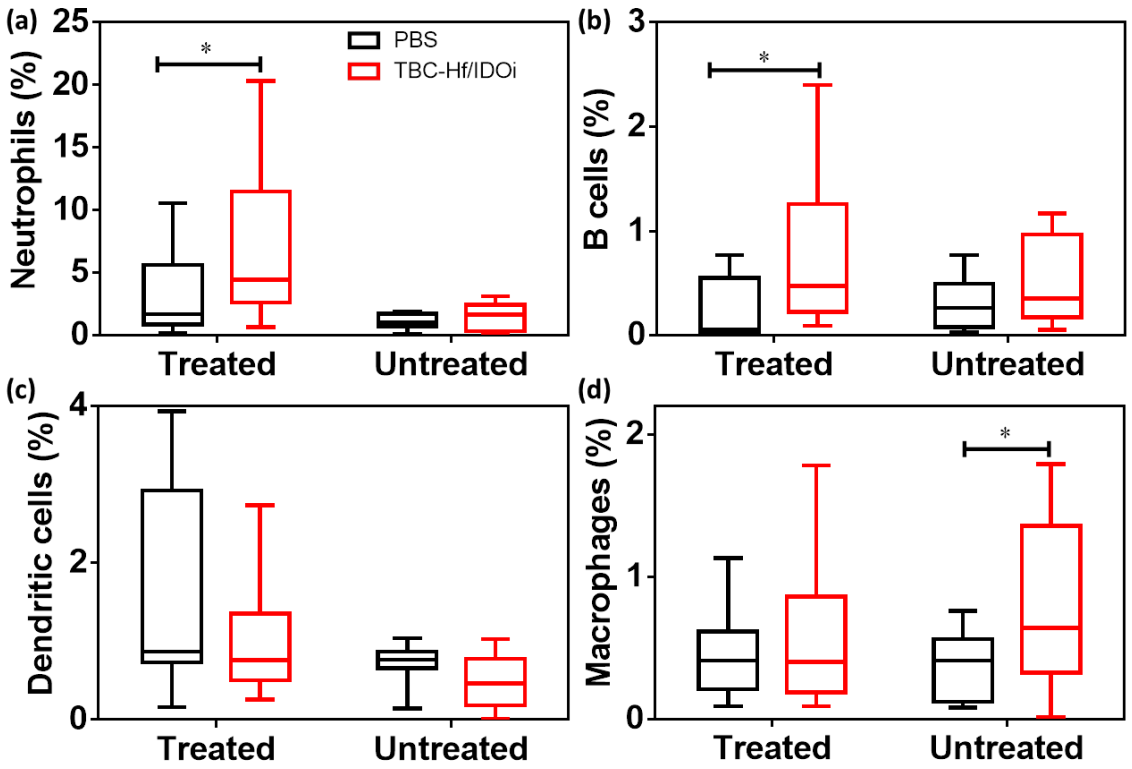

Figure S23. The percentage of tumor-infiltrating neutrophils (a), B cells (b), dendritic cells (c) and macrophages (d) with respect to the total number of cells in the tumor compared to PBS, 12h after IDOi@TBC-Hf PDT treatment.

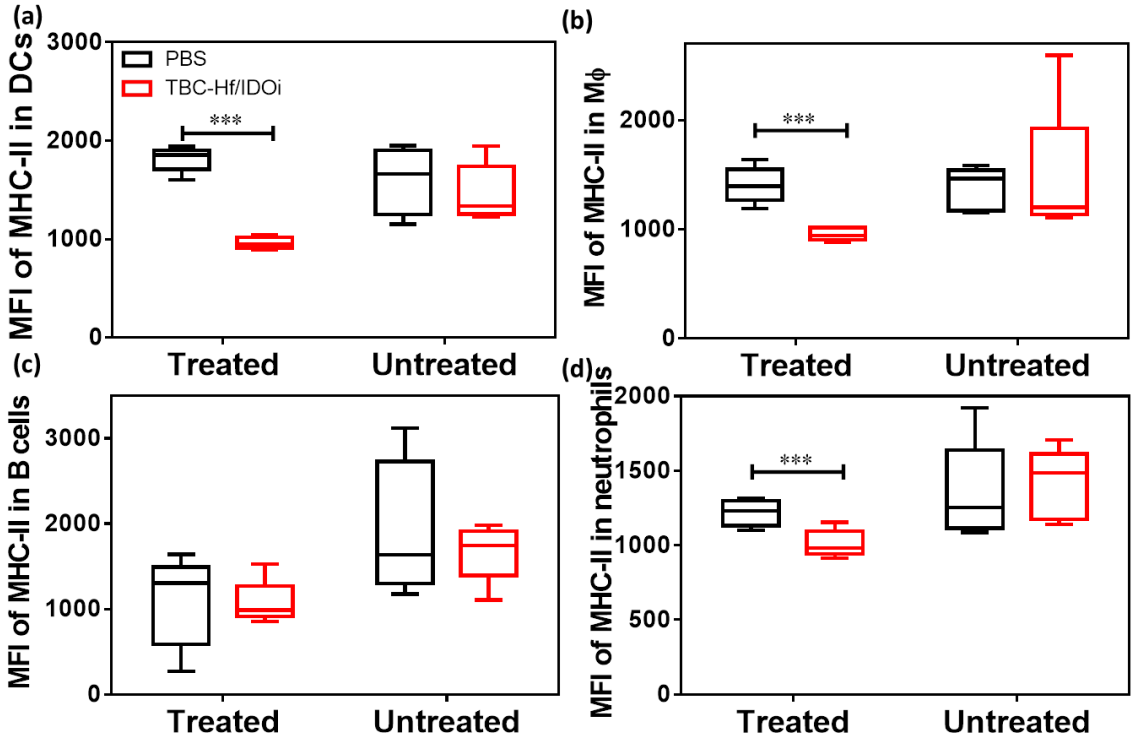

Figure S24. The MHC-II expression level in neutrophils, B cells, dendritic cells, and macrophages at 12 h after IDOi@TBC-Hf PDT treatment.

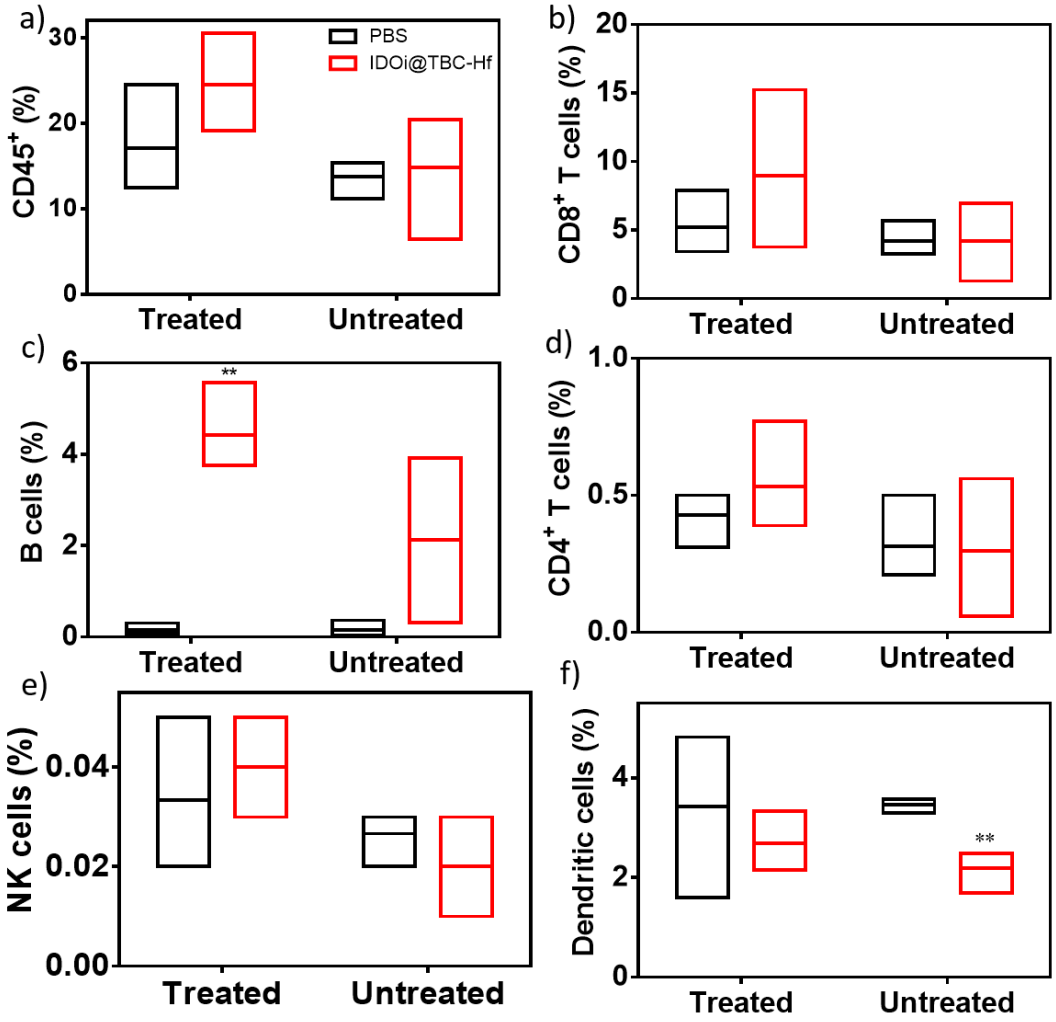

Figure S25. The percentage of tumor-infiltrating $CD45^+$ cells (a), $CD8^+$ T cells (b), B cells (c), $CD4^+$ T cells (d), NK cells (e) and dendritic cells (f) with respect to the total number of cells in the tumor compared to PBS, 7 days after IDOi@TBC-Hf PDT treatment.

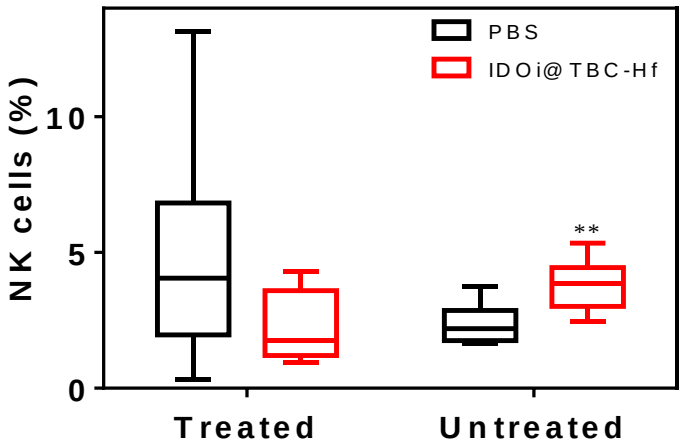

Figure S26. The tumor-infiltrating NK cells percentage with respect the total number of cells in the tumors at 12 days after IDOi@TBC-Hf PDT treatment.

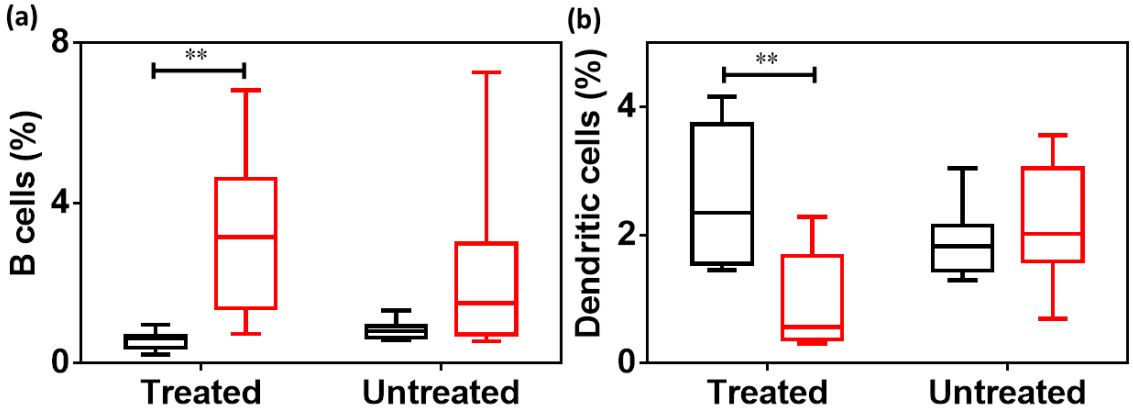

Figure S27. The tumor-infiltrating B cell (a) and dendritic cell (b) percentage with respect to the total number of cells in the tumors at 12 days after IDOi@TBC-Hf PDT treatment.